FINITE ELEMEMT ANALYSIS OF NON-DARCY MIXED CONVECTIVE HEAT AND MASS TRANSFER IN A CIRCULAR ANNULUS WITH RADIATION ABSORPTION

P.Sriveni[1] **Prof.A.Leelarathnam[2]**

Abstract: In this chapter we discuss the free and forced convection flow through a porous medium in a co-axial cylindrical duct where the boundaries are maintained at constant temperature and concentration. The Brinkman Forchhimer extended Darcy equations which take into account the boundary and inertia effects are used in the governing linear momentum equations. The effect of density variation is confined to the buoyancy term under Boussinesq approximation.

Index Terms: Radiation Absorption, chemical reaction.

1. INTRODUCTION

Transport phenomena involving the combined influence of thermal and concentration buoyancy are often encountered in many engineering systems and natural environments. There are many applications of such transport processes in the industry, notably in chemical distilleries, heat exchangers, solar energy collectors and thermal protection systems. In all such classes of flows, the driving force is provided by a combination of thermal and chemical diffusion effects. In atmosphere flows, thermal convection of the earth by sunlight is affected by differences in water vapour concentration. This buoyancy driven convection due to coupled heat and mass transfer in porous media has also many important applications in energy related engineering. These include moisture migration, fibrous insulation, spreading of chemical pollution in saturated soils, extraction of geothermal energy and underground disposal of natural waste.

The increasing cost of energy has led technologists to examine measures which could considerably reduce the usage of the natural source energy. Thermal insulations will continue to find increased use as engineers seek to reduce cost. Heat transfer in the porous thermal insulation within vertical cylindrical annuli provide us insight into the mechanism of energy transport and enable engineers to use insulation more efficiently. In particular, design engineers require relationships between heat transfer, geometry and boundary conditions which can be utilized in cost –benefit analysis to determine the amount of insulation that will yield the maximum investment. Apart from this, the study of flow and heat transfer in the annular region between the concentric cylinders has applications in nuclear waste disposal research. It is known that canisters filled with radioactive rays be buried in earth so as to isolate them from human population and it is of interest to determine the surface temperature of these canisters. This surface temperature strongly depends on the buoyancy driven flows sustained by the heated surface and the possible moment of ground water past it. This phenomenon is ideal to the study of convection flow in a porous medium contained in a cylindrical annulus (15, 16, 17).

Free convection in a vertical porous annulus has been extensively studied by Prasad (15), Prasad and Kulacki (16) and Prasad et al. (17) both theoretically and experimentally. Caltagirone (3) has published a detailed theoretical study of free convection in a horizontal porous annulus including possible three dimensional and transient effects. Convection through annulus region under steady state conditions has also been discussed with two cylindrical surfaces kept at different temperatures (7). This work has been extended in temperature dependent convection flow (5, 6, 7)as well as convection flows through horizontal porous channel whose inner surface is maintained at constant temperature while the other surface is maintained at circumferentially varying sinusoidal temperature (10, 19, 27).

Free convection flow and heat transfer in hydromagnetic case is important in nuclear and space technology (7, 11, 14, 22, 29, 30). In particular, such convection flow in a vertical annulus region in the presence of radial magnetic field has been studied by Sastri and Bhadram (20). Nanda and Purushotham (8) have analysed the free convection of a thermal conducting viscous incompressible fluid induced by travelling thermal waves on the circumference of a long vertical circular cylindrical pipe. Whitehead (28) and Neeraja (9) have made a study of the fluid flow and heat transfer in a viscous incompressible fluid confined in an annulus bounded by two rigid cylinders. The flow is generated by periodical travelling waves imposed on the outer cylinder and the inner cylinder is maintained at constant temperature.

Chen and Yuh (4) have investigated the heat and mass transfer characteristics of natural convection flow along a vertical cylinder under the combined buoyancy effects of thermal and species diffusion. Sivanjaneya Prasad (23) has investigated the free convection flow of an incompressible, viscous fluid through a porous medium in the annulus between the porous concentric cylinders under the influence of a radial magnetic field. Antonio (2)

has investigated the laminar flow, heat transfer in a vertical cylindrical duct by taking into account both viscous dissipation and the effect of buoyancy, The limiting case of fully developed natural convection in porous annuli is solved analytically for steady and transient cases by Sharawi and Al-Nimir (21) and Al-Nimir (1). Philip (13) has obtained solutions for the annular porous media valid for low modified Reynolds number. Ravi (18) has analysed the unsteady convective heat and mass transfer through a cylindrical annulus with constant heat sources. Sreevani (25) has studied the convective heat and mass transfer through a porous medium in a cylindrical annulus under radial magnetic field with Soret effect. Prasad (15) has analysed the convective heat and mass transfer in an annulus in the presence of heat generating source under radial magnetic field. Reddy (24) has discussed the Soret effect on mixed convective heat and mass transfer through a porous cylindrical annulus. For natural convection, the existence of large temperature differences between the surfaces is important. Keeping the applications in view, Sudheer Kumar et al. (26) have studied the effect of radiation on natural convection over a vertical cylinder in a porous media. Padmavathi (12) has analyzed the convective heat transfer in a cylindrical annulus by using finite element method.

In this chapter, we discuss the free and forced convection flow through a porous medium in a co-axial cylindrical duct where the boundaries are maintained at constant temperature and concentration. The Brinkman Forchhimer extended Darcy equations which take into account the boundary and inertia effects are used in the governing linear momentum equations. The effect of density variation is confined to the buoyancy term under Boussinesq approximation. The momentum, energy and diffusion equations are coupled equations. In order to obtain a better insight into this complex problem, we make use of Galerkin finite element analysis with quadratic polynomial approximations. The Galerkin finite element analysis has two important features. The first is that the approximation solution is written directly as a linear combination of approximation functions with unknown nodal values as coefficients. Secondly, the approximation polynomials are chosen exclusively from the lower order piecewise polynomials restricted to contiguous elements. The behaviour of velocity, temperature and concentration is analysed at different axial positions. The shear stress and the rate of heat and mass transfer have also been obtained for variations in the governing parameters.

SCHEMATIC DIAGRAM OF THE CONFIGURATION

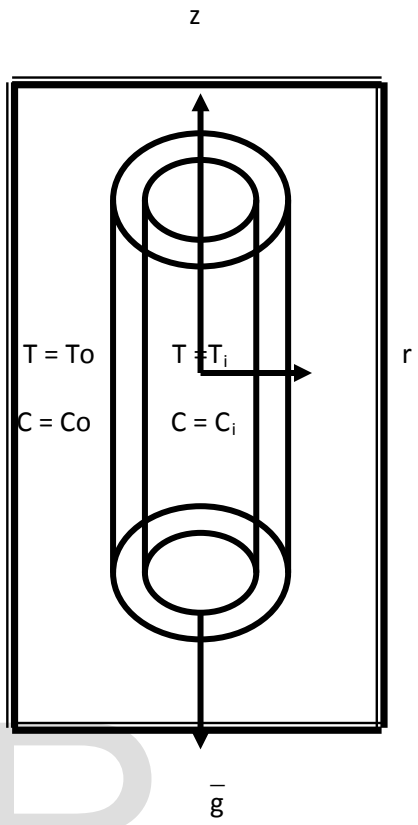

3. FORMULATION OF THE PROBLEM

We consider the free and forced convection flow in a vertical circular annulus through a porous medium whose walls are maintained at constant temperature and concentration. The flow, temperature and concentration in the fluid are assumed to be fully developed. Both the fluid and porous regions have constant physical properties and the flow is a mixed convection flow taking place under thermal and molecular buoyancies and uniform axial pressure gradient. The Boussenissq approximation is invoked so that the density variation is confined to the thermal and molecular buoyancy forces. The Brinkman-Forchhimer-Extended Darcy model which accounts for the inertia and boundary effects has been used for the momentum equation in the porous region. The momentum, energy and diffusion equations are coupled and non-linear. Also the flow is unidirectional along the axial direction of the cylindrical annulus. Making use of the above assumptions the governing equations are

$$-\frac{\partial p}{\partial z}+\frac{\mu}{\delta}\left(\frac{\partial^2 u}{\partial r^2}+\frac{1}{r}\frac{\partial u}{\partial r}\right)-\frac{\mu}{k}u+\rho g\beta(T-T_0) + \rho g\beta^{\bullet}(C-C_0)+\frac{\delta u^2}{\sqrt{k}}=0 \qquad (2.1)$$

[1]Dept. of Applied Mathematics, SPMVV, Tirupati, A.P.
Email id:parvathimani2008@gmail.com
[2]Dept. of Applied Mathematics, SPMVV, Tirupati, A.P.
Email id:maherahul.55@gmail.com

$$\rho c_p u \frac{\partial T}{\partial z} = \lambda\left(\frac{\partial^2 T}{\partial r^2} + \frac{1}{r}\frac{\partial T}{\partial r}\right) + Q(T_0 - T) + Q_1^{'} C \qquad (2.2)$$

$$u\frac{\partial C}{\partial z} = D_1\left(\frac{\partial^2 C}{\partial r^2} + \frac{1}{r}\frac{\partial C}{\partial r}\right) - kC \qquad (2.3)$$

where u is the axial velocity in the porous region, T, C are the temperature and concentration of the fluid, k is the permeability of porous medium, F is a function that depends on Reynolds number, the microstructure of the porous medium and D_1 is the molecular diffusivity, β is the coefficient of the thermal expansion, β* is the coefficient of volume expansion, C_p is the specific heat, ρ is density and g is gravity.

The relevant boundary conditions are

$u = 0$, T=T_i, C= C_i at r = a

$u = 0$, T=T_0, C=C_0 at r = a+s (2.4)

We now define the following non-dimensional variables

$$z^* = \frac{z}{a}\ ,\quad r^* = \frac{r}{a}\ ,\quad u^* = \frac{a}{\gamma}u$$

$$p^* = \frac{pa\delta}{\rho\gamma^2}\ ,\quad \theta^* = \frac{T - T_0}{T_i - T_0}\ ,\quad s^* = \frac{s}{a}$$

$$C^* = \frac{C - C_0}{C_i - C_0}$$

Introducing these non-dimensional variables, the governing equations in the non-dimensional form are (on removing the stars)

$$\frac{\partial^2 u}{\partial r^2} + \frac{1}{r}\frac{\partial u}{\partial r} = \pi + \delta(D^{-1})u + \delta^2\Lambda u^2 - \delta G(\theta + N\,C) \qquad (2.5)$$

$$\frac{\partial^2 \theta}{\partial r^2} + \frac{1}{r}\frac{\partial \theta}{\partial r} - \alpha\,\theta = P_r N_1 u - Q_1 C \qquad (2.6)$$

$$\frac{\partial^2 C}{\partial r^2} + \frac{1}{r}\frac{\partial C}{\partial r} - \gamma\, C = Sc\, N_2 u \qquad (2.7)$$

Where $\Lambda = FD^{-1}$ (Inertia parameter or Forchhimer number)

$$G = \frac{g\beta(T_1 - T_0)a^3}{\gamma^2}$$ (Grashof number)

$$D^{-1} = \frac{a^2}{k}$$ (Inverse Darcy parameter)

$$N_1 = \frac{Aa}{T_1 - T_0}$$ (Non-dimensional temperature gradient)

$$N_2 = \frac{Ba}{C_1 - C_0}$$ (Non-dimensional concentration gradient)

$$P_r = \frac{\rho c_p \gamma}{\lambda}$$ (Prandtl number)

$$Sc = \frac{\nu}{D_1}$$ (Schmidt number)

$$\gamma = \frac{ka^2}{D_1}$$ (Chemical reaction parameter)

$$Q_1 = \frac{Q_1^{'}(C_i - C_0)a^2}{\lambda C_p(T_i - T_0)}$$ (Radiation absorption parameter)

$$\pi = \frac{\partial P}{\partial Z}$$

The corresponding non-dimensional conditions are

$u = 0, \theta = 1,$ C=1 at r=1

$u = 0, \theta = 0,$ C=0 at r=1+s (2.8)

For N=0 the equations (2.5) – (2.7) reduce to that of padmavathi (12)

For $\alpha = 0$ they are in good agreement with Sudha (31)

4. FINITE ELEMENT ANALYSIS

The finite element analysis with quadratic polynomial approximation functions is carried out along the radial distance across the circular duct. The behaviour of the velocity, temperature and concentration profiles has been discussed computationally for different variations in governing parameters. The Galerkin method has been adopted in the variational formulation in each element to obtain the global coupled matrices for the velocity, temperature and concentration in course of the finite element analysis.

Choose an arbitrary element E_k and let u^k, θ^k and C^k be the values of u, θ and C in the element E_k

We define the error residuals as

$$E_p^k = \frac{d}{dr}\left(r\frac{du^k}{dr}\right) + \delta G(\theta^k + NC^k) - \delta(D^{-1})ru^k - \delta^2\Lambda r(u^k)^2 \quad (3.1)$$

$$E^k{}_\theta = \frac{d}{dr}\left(r\frac{d\theta^k}{dr}\right) - rP_rN_1u^k - \alpha r\theta^k + Q_1 rC^k \quad (3.2)$$

$$E^k{}_c = \frac{d}{dr}\left(r\frac{dC^k}{dr}\right) - \gamma rC^k - rScN_2u^k \quad (3.3)$$

where u^k, θ^k & C^k are values of u, θ & C in the arbitrary element e_k. These are expressed as linear combinations in terms of respective local nodal values.

$$u^k = u_1^k\psi_1^k + u_3^k\psi_1^k + u_3^k\psi_3^k$$

$$\theta^k = \theta_1^k\psi_1^k + \theta_2^k\psi_2^k + \theta_3^k\psi_3^k$$

$$C^k = C_1^k\psi_1^k + C_2^k\psi_2^k + C_3^k\psi_3^k$$

where ψ_1^k, ψ_2^k --------- etc are Lagrange's quadratic polynomials.

Following the Galerkin weighted residual method and integrating by parts equations (3.1) - (3.3) we obtain

$$\int_{rA_1}^{rB_1} r\frac{du^k}{dr}\frac{d\psi_j^k}{dr}dr - \delta G\int_{rA_1}^{rB_1} r(\theta^k + NC^k)\psi_j^k dr + \delta(M_1{}^2)\int_{rA_1}^{rB_1} ru^k\psi_j^k dr + \delta^2\Lambda\int_{rA_1}^{rB_1} r(u^k)^2\psi_j^k dr$$
$$= Q_{2\,j}^k + Q_{1\,j}^k - P\int_{rA_1}^{rB_1} r\psi_j^k dr \quad (3.4)$$

$$-Q_{1\,j}^k = \left[\left(\frac{du^k}{dr}\right)(r\psi_j^k)\right]r_{A_1},$$

$$-Q_{2\,j}^k = \left[\left(\frac{du^k}{dr}\right)(r\psi_j^k)\right]r_{B_1}$$

$$\int_{rA_1}^{rB_1} r\frac{du^k}{dr}\frac{d\psi_j{}^k}{dr}dr = N_1P_r\int_{rA_1}^{rB_1} ru^k\psi_j^k dr + R_{2\,j}^k + R_{1\,j}^k \quad (3.5)$$

$$-R_{1\,j}^k = \left[\left(\frac{d\theta^k}{dr}\right)(r\psi_j^k)\right]r_{A_1},$$

$$R_{2\,j}^k = \left[\left(\frac{d\theta^k}{dr}\right)(r\psi_j^k)\right]r_{B_1}$$

$$\int_{rA_1}^{rB_1} r\frac{du^k}{dr}\frac{d\psi_j{}^k}{dr}dr = N_2Sc\int_{rA_1}^{rB_1} ru^k\psi_j^k dr + S_{2\,j}^k + S_{1\,j}^k \quad (3.6)$$

$$-S_{1\,j}^k = \left[\left(\frac{dC^k}{dr}\right)(r\psi_j^k)\right]r_{A_1},$$

$$S_{2\,j}^k = \left[\left(\frac{dC^k}{dr}\right)(r\psi_j^k)\right]r_{B_1}$$

Expressing u^k, θ^k, C^k in terms of local nodal values in (3.4) - (3.6) we obtain

$$\sum_{i=1}^3 u^k\int_{rA_1}^{rB_1} r\frac{d\psi_i^k}{dr}\frac{d\psi_j^k}{dr}dr - \delta G\sum_{i=1}^3(\theta_i^k + NC_i^k)\int_{rA_1}^{rB_1} r\psi_i^k\psi_j^k dr + \delta D^{-1}\sum_{i=1}^3\int_{rA_1}^{rB_1} r\psi_i^k\psi_j^k dr$$
$$+ \delta^2\Lambda\sum_{i=1}^3 u_i^k\int_{rA_1}^{rB_1} rU_i^k\psi_i^k\psi_j^k dr = Q_{2\,j}^j + Q_{1\,j}^k - P\int_{rA_1}^{rB_1} r\psi_i^k\psi_j^k dr \quad (3.7)$$

$$\sum_{i=1}^3\theta_i^k\int_{rA_1}^{rB_1} r\frac{d\psi_i^k}{dr}\frac{d\psi_j^k}{dr}dr - N_1P_r\sum_{i=1}^3 u_i^k\int_{rA_1}^{rB_1} r\psi_i^k\psi_j^k dr + \alpha\int_{rA_1}^{rB_1}\theta dr - Q_1\sum_{i=1}^3 C_i^k\int_{rA_1}^{rB_1} r\psi_j^k dr = R_{2\,j}^k + R_{1\,j}^k \quad (3.8)$$

$$\sum_{i=1}^3 C_i^k\int_{rA_1}^{rB_1} r\frac{d\psi_i^k}{dr}\frac{d\psi_j^k}{dr}dr - N_2Sc\sum_{i=1}^3 u_i^k\int_{rA_1}^{rB_1} r\psi_i^k\psi_j^k dr - \gamma\sum_{i=1}^3 C_i^k\int_{rA_1}^{rB_1} r\psi_j^k\, dr = S_{2\,j}^k + S_{1\,j}^k \quad (3.9)$$

$$M_1^2 = D^{-1} + M^2 \quad (3.9a)$$

Choosing different ψ_j^k's corresponding to each element e_k in the equation (3.7) yields a local stiffness matrix of order 3×3 in the form

$$(f_i^k{}_j)(u_i^k) - \delta G(g_i^k{}_j)(\theta_i^k + NC_i^k) + \delta D^{-1}(m_i^k{}_j)(u_i^k) + \delta^2\Lambda(n_i^k{}_j)(u_i^k) = (Q_{2\,j}^k) + (Q_{1\,j}^k) + (v_j^k) \quad (3.10)$$

Likewise the equations (3.8) & (3.9) give rise to stiffness matrices

$$(e_i^k{}_j)(\theta_i^k) - N_1P_r(t_i^k{}_j)(u_i^k) + Q_1(C_i^k) = R_{2\,j}^k + R_{1\,j}^k \quad (3.11)$$

$$(l_i^k{}_j)(C_i^k) - N_2c(t_i^k{}_j)(u_i^k) - \gamma(C_i^k) = S_{2\,j}^k + S_{1\,j}^k \quad (3.12)$$

where

$(f_{i\ j}^{k})$, $(g_{i\ j}^{k})$, $(m_{i\ j}^{k})$, $(n_{i\ j}^{k})$, $(e_{i\ j}^{k})$, $(l_{i\ j}^{k})$ and $(t_{i\ j}^{k})$ are 3×3 matrices and $v_j^k = -P_1 \int_{rA_1}^{rB_1} r\psi_i^k \psi_j^k dr$

and $(Q_{2\ j}^{k})$, $(Q_{1\ j}^{k})$, $(R_{2\ j}^{k})$ & $(R_{1\ j}^{k})$, $(S_{2\ j}^{k})$ & $(S_{1\ j}^{k})$ are 3×1 column matrices. Such stiffness matrices (3.10) - (3.12) in terms of local nodes in each element are assembled using interelement continuity and equilibrium conditions to obtain the coupled global matrices in terms of the global nodal values of u , θ & C in the region.

In case we choose n quadratic elements, then the global matrices are of order 2n+1. The ultimate coupled global matrices are solved to determine the unknown global nodal values of the velocity, temperature and concentration in fluid region. In solving these global matrices an iteration procedure has been adopted to include the boundary effects in the porous medium.

In fact, the non-linear term arises in the modified Brinkman linear momentum equation (3.4) of the porous medium. The iteration procedure in taking the global matrices is as follows. We split the square term into a product term and keeping one of them say U_i's under integration, the other is expanded in terms of local nodal values as in (3.7), resulting in the corresponding coefficient matrix $(n_{i\ j}^{k}{}'s)$ in (3.10), whose coefficients involve the unknown u_i's . To evaluate (3.10), to begin with, choose the initial global nodal values of u_i's as zeros in the zeroth approximation. We evaluate u_i's, θ_i's and C_i's in the usual procedure mentioned earlier. Later choosing these values of u_i's as first order approximation calculate θ_i's, C_i's. In the second iteration, we substitute for u_i's the first order approximation of u_i's and the first approximation of θ_i's and C_i's and obtain second order approximation. This procedure is repeated till the consecutive values of u_i's, θ_i's and C_i's differ by a preassigned percentage.

For computational purpose we choose five elements in flow region

The shape functions in the region are

$$\psi_1^1 = \frac{50(-1+r-\frac{s}{5})(-1+r-\frac{s}{10})}{s^2}$$

$$\psi_2^1 = \frac{100(-1+r)(-1+r-\frac{s}{5})}{s^2}$$

$$\psi_3^1 = \frac{50(-1+r)(-1+r-\frac{s}{10})}{s^2}$$

$$\psi_1^2 = \frac{50(-1+r-\frac{2s}{5})(-1+r-\frac{3s}{10})}{s^2}$$

$$\psi_2^2 = -\frac{100(-1+r-\frac{2s}{5})(-1+r-\frac{s}{5})}{s^2}$$

$$\psi_3^2 = \frac{50(-1+r-\frac{3s}{5})(-1+r-\frac{s}{5})}{s^2}$$

$$\psi_1^3 = \frac{50(-1+r-\frac{3s}{5})(-1+r-\frac{s}{2})}{s^2}$$

$$\psi_2^3 = -\frac{100(-1+r-\frac{3s}{5})(-1+r-\frac{2s}{5})}{s^2}$$

$$\psi_3^3 = \frac{50(-1+r-\frac{s}{2})(-1+r-\frac{2s}{5})}{s^2}$$

$$\psi_1^4 = \frac{50(-1+r-\frac{4s}{5})(-1+r-\frac{7s}{10})}{s^2}$$

$$\psi_2^4 = -\frac{100(-1+r-\frac{4s}{5})(-1+r-\frac{3s}{5})}{s^2}$$

$$\psi_3^4 = \frac{50(-1+r-\frac{7s}{10})(-1+r-\frac{3s}{5})}{s^2}$$

$$\psi_1^5 = \frac{50(-1+r-s)(-1+r-\frac{9s}{10})}{s^2}$$

$$\psi_2^5 = -\frac{100(-1+r-s)(-1+r-\frac{4s}{5})}{s^2}$$

$$\psi_3^5 = \frac{50(-1+r-\frac{9s}{10})(-1+r-\frac{4s}{5})}{s^2}$$

The global matrix for θ is

$$A_3 X_3 = B_3 \qquad (3.13)$$

The global matrix for C is

$$A_4 X_4 = B_4 \qquad (3.14)$$

The global matrix for u is

$$A_5 X_5 = B_5 \qquad (3.15)$$

Where

$$A_3 = \begin{bmatrix} e_{11} & e_{12} & e_{13} & 0 & 0 & 0 & 0 & 0 & 0 & 0 & 0 \\ e_{21} & e_{22} & e_{23} & 0 & 0 & 0 & 0 & 0 & 0 & 0 & 0 \\ e_{31} & e_{32} & e_{33} & e_{34} & e_{35} & 0 & 0 & 0 & 0 & 0 & 0 \\ 0 & 0 & e_{43} & e_{44} & e_{45} & 0 & 0 & 0 & 0 & 0 & 0 \\ 0 & 0 & e_{53} & e_{54} & e_{55} & e_{56} & e_{57} & 0 & 0 & 0 & 0 \\ 0 & 0 & 0 & 0 & e_{65} & e_{66} & e_{67} & 0 & 0 & 0 & 0 \\ 0 & 0 & 0 & 0 & e_{75} & e_{76} & e_{77} & e_{78} & e_{79} & 0 & 0 \\ 0 & 0 & 0 & 0 & 0 & 0 & e_{87} & e_{88} & e_{89} & 0 & 0 \\ 0 & 0 & 0 & 0 & 0 & 0 & e_{97} & e_{98} & e_{99} & e_{910} & e_{911} \\ 0 & 0 & 0 & 0 & 0 & 0 & 0 & 0 & e_{109} & e_{1010} & e_{1011} \\ 0 & 0 & 0 & 0 & 0 & 0 & 0 & 0 & e_{119} & e_{1110} & e_{1111} \end{bmatrix}$$

$$A_4 = \begin{bmatrix} k_{11} & k_{12} & k_{13} & 0 & 0 & 0 & 0 & 0 & 0 & 0 & 0 \\ k_{21} & k_{22} & k_{23} & 0 & 0 & 0 & 0 & 0 & 0 & 0 & 0 \\ k_{31} & k_{32} & k_{33} & k_{34} & k_{35} & 0 & 0 & 0 & 0 & 0 & 0 \\ 0 & 0 & k_{43} & k_{44} & k_{45} & 0 & 0 & 0 & 0 & 0 & 0 \\ 0 & 0 & k_{53} & k_{54} & k_{55} & k_{56} & k_{57} & 0 & 0 & 0 & 0 \\ 0 & 0 & 0 & 0 & k_{65} & k_{66} & k_{67} & 0 & 0 & 0 & 0 \\ 0 & 0 & 0 & 0 & k_{75} & k_{76} & k_{77} & k_{78} & k_{79} & 0 & 0 \\ 0 & 0 & 0 & 0 & 0 & 0 & k_{87} & k_{88} & k_{89} & 0 & 0 \\ 0 & 0 & 0 & 0 & 0 & 0 & k_{97} & k_{98} & k_{99} & k_{910} & k_{911} \\ 0 & 0 & 0 & 0 & 0 & 0 & 0 & 0 & k_{109} & k_{1010} & k_{1011} \\ 0 & 0 & 0 & 0 & 0 & 0 & 0 & 0 & k_{119} & k_{1110} & k_{1111} \end{bmatrix}$$

$$A_5 = \begin{bmatrix} h_{11} & h_{12} & h_{13} & 0 & 0 & 0 & 0 & 0 & 0 & 0 & 0 \\ h_{21} & h_{22} & h_{23} & 0 & 0 & 0 & 0 & 0 & 0 & 0 & 0 \\ h_{31} & h_{32} & h_{33} & h_{34} & h_{35} & 0 & 0 & 0 & 0 & 0 & 0 \\ 0 & 0 & h_{43} & h_{44} & h_{45} & 0 & 0 & 0 & 0 & 0 & 0 \\ 0 & 0 & h_{53} & h_{54} & h_{55} & h_{56} & h_{57} & 0 & 0 & 0 & 0 \\ 0 & 0 & 0 & 0 & h_{65} & h_{66} & h_{67} & 0 & 0 & 0 & 0 \\ 0 & 0 & 0 & 0 & h_{75} & h_{76} & h_{77} & h_{78} & h_{79} & 0 & 0 \\ 0 & 0 & 0 & 0 & 0 & 0 & h_{87} & h_{88} & h_{89} & 0 & 0 \\ 0 & 0 & 0 & 0 & 0 & 0 & h_{97} & h_{98} & h_{99} & h_{910} & h_{911} \\ 0 & 0 & 0 & 0 & 0 & 0 & 0 & 0 & h_{109} & h_{1010} & h_{1011} \\ 0 & 0 & 0 & 0 & 0 & 0 & 0 & 0 & h_{119} & h_{1110} & h_{1111} \end{bmatrix}$$

$$h_{ij} = f_{ij} + \delta D^{-1} m_{ij} + \delta^2 \Lambda n_{ij}$$

$$X_3 = \begin{bmatrix} \theta_1 \\ \theta_2 \\ \theta_3 \\ \theta_4 \\ \theta_5 \\ \theta_6 \\ \theta_7 \\ \theta_8 \\ \theta_9 \\ \theta_{10} \\ \theta_{11} \end{bmatrix} \quad X_4 = \begin{bmatrix} C_1 \\ C_2 \\ C_3 \\ C_4 \\ C_5 \\ C_6 \\ C_7 \\ C_8 \\ C_9 \\ C_{10} \\ C_{11} \end{bmatrix} \quad X_5 = \begin{bmatrix} u_1 \\ u_2 \\ u_3 \\ u_4 \\ u_5 \\ u_6 \\ u_7 \\ u_8 \\ u_9 \\ u_{10} \\ u_{11} \end{bmatrix}$$

$$B_3 = \begin{bmatrix} F_u^1 \\ F_u^2 \\ F_u^3 \\ F_u^4 \\ F_u^5 \\ F_u^6 \\ F_u^7 \\ F_u^8 \\ F_u^9 \\ F_u^{10} \\ F_u^{11} \end{bmatrix} \quad B_4 = \begin{bmatrix} F_c^1 \\ F_c^2 \\ F_c^3 \\ F_c^4 \\ F_c^5 \\ F_c^6 \\ F_c^7 \\ F_c^8 \\ F_c^9 \\ F_c^{10} \\ F_c^{11} \end{bmatrix} \quad B_5 = \begin{bmatrix} F_\theta^1 \\ F_\theta^2 \\ F_\theta^3 \\ F_\theta^4 \\ F_\theta^5 \\ F_\theta^6 \\ F_\theta^7 \\ F_\theta^8 \\ F_\theta^9 \\ F_\theta^{10} \\ F_\theta^{11} \end{bmatrix}$$

(The details of e_{11} etc., h_{11} et., F_u^1 etc., F_θ^1 etc., F_c^1 are given in the appendix).

The equilibrium conditions are

$$R_3^1 + R_1^2 = 0, \qquad R_3^2 + R_1^3 = 0,$$

$$R_3^3 + R_1^4 = 0, \qquad R_3^4 + R_1^5 = 0,$$

$$Q_3^1 + Q_1^2 = 0, \qquad Q_3^2 + Q_1^3 = 0,$$

$$Q_3^3 + Q_1^4 = 0, \qquad Q_3^4 + Q_1^5 = 0,$$

$$S_3^1 + S_1^2 = 0, \qquad S_3^2 + S_1^3 = 0,$$

$$S_3^3 + S_1^4 = 0, \qquad S_3^4 + S_1^5 = 0, \qquad (3.16)$$

5. SOLUTION OF THE PROBLEM

Solving these coupled global matrices for temperature, concentration and velocity (3.13)-(3.15) respectively and using the iteration procedure we determine the unknown global nodes through which the temperature, concentration and velocity at different radial intervals at any arbitrary axial cross sections are obtained. The respective expressions are given by

$$\theta(r) = \psi_1^1\,\theta_{11} + \psi_{21}^1\,\theta_{12} + \psi_3^1\,\theta_{13}$$
$$1 \le r \le 1 + S*0.2$$
$$= \psi_1^2\,\theta_{13} + \psi_2^2\,\theta_{14} + \psi_3^2\,\theta_{15}$$

$$1 + S*0.2 \le r \le 1 + S*0.4$$

$$= \psi_1^3\,\theta_{15} + \psi_2^3\,\theta_{16} + \psi_3^3\,\theta_{17}$$

$$1 + S*0.4 \le r \le 1 + S*0.6$$

$$= \psi_1^4\,\theta_{17} + \psi_2^4\,\theta_{18} + \psi_3^4\,\theta_{19}$$
$$1 + S*0.6 \le r \le 1 + S*0.8$$

$$= \psi_1^{15}\,\theta_{19} + \psi_2^5\,\theta_{20} + \psi_3^5\,\theta_{21}$$

$$1 + S*0.8 \le r \le 1 + S$$

$$C(r) = \psi_1^1\,C_{11} + \psi_{21}^1\,C_{12} + \psi_3^1\,C_{13}$$
$$1 \le r \le 1 + S*0.2$$
$$= \psi_1^2\,C_{13} + \psi_2^2\,C_{14} + \psi_3^2\,C_{15}$$

$$1 + S*0.2 \le r \le 1 + S*0.4$$

$$= \psi_1^3\,C_{15} + \psi_2^3\,C_{16} + \psi_3^3\,C_{17}$$

$$1 + S*0.4 \le r \le 1 + S*0.6$$

$$= \psi_1^4\,C_{17} + \psi_2^4\,C_{18} + \psi_3^4\,C_{19}$$
$$1 + S*0.6 \le r \le 1 + S*0.8$$

$$= \psi_1^{15}\,C_{19} + \psi_2^5\,C_{20} + \psi_3^5\,C_{21}$$
$$1 + S*0.8 \le r \le 1 + S$$

$$u(r) = \psi_1^1\,u_{11} + \psi_{21}^1\,u_{12} + \psi_3^1\,u_{13}$$
$$1 \le r \le 1 + S*0.2$$

$$= \psi_1^2\,u_{13} + \psi_2^2\,u_{14} + \psi_3^2\,u_{15}$$
$$1 + S*0.2 \le r \le 1 + S*0.4$$

$$= \psi_1^3\,c_{15} + \psi_2^3\,c_{16} + \psi_3^3\,c_{17}$$
$$1 + S*0.4 \le r \le 1 + S*0.6$$

$$= \psi_1^4\,u_{17} + \psi_2^4\,u_{18} + \psi_3^4\,u_{19}$$
$$1 + S*0.6 \le r \le 1 + S*0.8$$

$$= \psi_1^{15}\,u_{19} + \psi_2^5\,u_{20} + \psi_3^5\,u_{21}$$
$$1 + S*0.8 \le r \le 1 + S$$

6. SHEAR STRESS, NUSSELT NUMBER AND SHERWOOD NUMBER

The shear stress (τ) is evaluated using the formula

$$\tau = \left(\frac{du}{dr}\right)_{r=1,1+s}$$

The rate of heat transfer (Nusselt number) is evaluated using the formula $Nu = -\left(\frac{d\theta}{dr}\right)_{r=1,1+s}$

The rate of mass transfer (Sherwood number) is evaluated using the formula $Sh = -\left(\frac{dC}{dr}\right)_{r=1,1+s}$

7. DISCUSSION OF THE NUMERICAL RESULTS

In this analysis we investigate the effect of chemical reaction and radiation absorption on convective heat and mass transfer flow of a viscous electrically conducting fluid through a porous medium in a circular annular region between the two porous cylinders r = a and r = b. The equations governing flow, heat and mass transfer are solved by using Gauss-Seidel iteration method.

The axial velocity (w) is shown in figs. (1-6) for different variations, G, D^{-1}, α, N, Sc, γ and Q_1. Fig. (1) represents w with Grashof number G. The actual axial flow is in the direction of gravitational field. W>0 represents a reversal flow. It is found that w exhibits a reversal flow for G<0 and the region of reversal flow enlarges with |G| with maximum occurring at r = 1.6. Fig. (2) represents w with D^{-1} and M. It is found that lesser the permeability of the porous medium lesser is |w| in the flow region. |w| experiences an enhancement with M≤4 and reduces with higher M≥6. An increase in the strength of the heat source results in a depreciation in |w|. The variation of w with buoyancy ratio N shows that when the molecular buoyancy force dominates over the thermal buoyancy force |w| enhances and when the buoyancy forces are in the same direction and for the forces acting in opposite directions |w| depreciates in the entire flow region fig. (3). The variation of w with Sc shows that |w| depreciates with Sc. Thus lesser the molecular diffusivity smaller is |w| in the flow region. The variation of w with chemical reaction parameter shows that |w| depreciates in the degenerating chemical reaction case and enhances in the generating chemical reaction case as shown in fig. (4). An increase in the radiation absorption parameter Q_1 results in an enhancement in |w| as presented in fig. (5).

The non-dimensional temperature (θ) is shown in figs. (6-10) for different parametric values. We assume that the outer cylinder is at a higher temperature than the inner cylinder (m=2). Fig. (6) represents the variation of θ with Grashof number G. It is found that the actual temperature depreciates with increase in |G|. The variation of θ with D^{-1} and M shows that lesser the permeability of the porous medium larger is the actual temperature. Higher the Lorentz force lesser the actual temperature in the flow region fig. (7). An increase in the strength of the heat source results in a depreciation of the actual temperature. When the molecular buoyancy force dominates over the thermal buoyancy force the actual temperature depreciates irrespective of the directions of the buoyancy forces as seen in fig. (8). With reference to Sc we find that lesser the molecular diffusivity smaller is the actual temperature. Also the actual temperature enhances in the generating chemical reaction case and depreciates in the degenerating chemical reaction case as observed from fig. (9). From fig. (10) we find that the actual temperature enhances with increase in the radiation absorption parameter Q_1.

The non-dimensional concentration (C) is shown in fig. (11) for different values of Sc and γ. It is found that lesser the molecular diffusivity smaller is the actual concentration. Also the actual concentration depreciates in the degenerating chemical reaction case and enhances in the generating chemical reaction case.

The shear stress (τ) on the inner and outer cylinders is shown in tables (1-8) for different values of G, D^{-1}, Sc, α, N, γ and Q_1. It is found that the stress enhances with |G| on both the cylinders. Lesser the permeability of the porous medium/higher the Lorentz force smaller is the stress on the boundaries. We find that the stress reduces with increase in the Schmidt number (Sc) tables (1 & 2). The stress depreciates with increase in the strength of the heat generating source. When the molecular buoyancy force dominates over the thermal buoyancy force the stress experiences depreciation irrespective of the directions of the buoyancy forces tables (3 & 4). With respect to the chemical reaction parameter γ we find that the stress depreciates in the degenerating chemical reaction case and enhances in the generating chemical reaction case tables (5 & 6). An increase in Q_1 leads to an enhancement in $|\tau|$ at both the cylinders as observed from tables (7 & 8).

The rate of heat transfer (Nu) at r = 1 & 2 is shown in tables (9-16) for different parametric values. It is found that the rate of heat transfer depreciates at r=1 and enhances at r = 2 with increase in G, M, D^{-1}, and λ. Thus lesser the permeability of the porous medium/higher Lorentz force, smaller |Nu| at r = 1 and larger $|\tau|$ at r = 2. Lesser the molecular diffusivity, smaller |Nu| is at r=1 and larger at r=2 tables (9 & 10). The variation of Nu with heat source parameter α shows that Nu at r = 1 reduces with $\alpha \leq 4$ and enhances with higher $\alpha \geq 6$ while at r = 2, it enhances with α. The rate of heat transfer enhances at r = 1 and depreciates at r = 2 with increase in |N| irrespective of the directions of the buoyancy forces tables (11 & 12). The Nusselt number at r = 1 depreciates and that at r = 2 enhances in the degenerating chemical reaction case while in the generating case it enhances on r = 1 and reduces on r = 2 tables (13 & 14). The Nusselt number on r = 1 enhances with increase in the radiation absorption parameter Q_1 while on r =2, it reduces with $Q_1 \leq 2$ and enhances with $Q_1 \geq 4$ tables (15 & 16).

The rate of mass transfer (Sh) depreciates on r = 1 and enhances on r=2 in the degenerating chemical reaction case and in the generating chemical reaction case it enhances on r=1 and reduces on r = 2 tables (17 & 18).

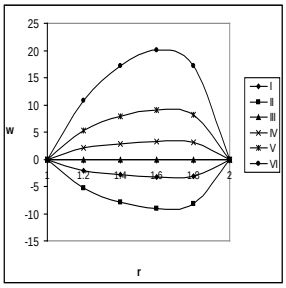

Fig. 1: Variation of w with G

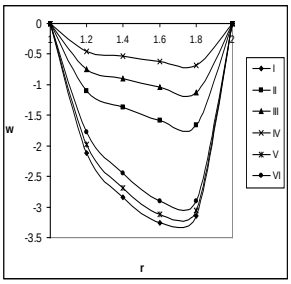

Fig. 2 : Variation of w with D^{-1},

	I	II	III	IV	V	VI
G	10^2	$2x10^2$	$3x10^2$	-10^2	$-2x10^2$	$-3x10^2$

	I	II	III	IV	V	VI
D^{-1}	10^2	$2x10^2$	$3x10^2$	$5x10^2$	10^2	10^2
M	2	2	2	2	4	6

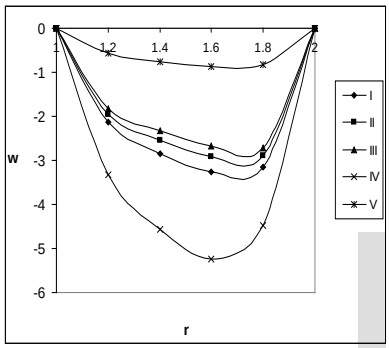

Fig. 3 : Variation of w with α, N

	I	II	III	IV	V
α	2	4	6	2	2
N	1	1	1	2	-0.5

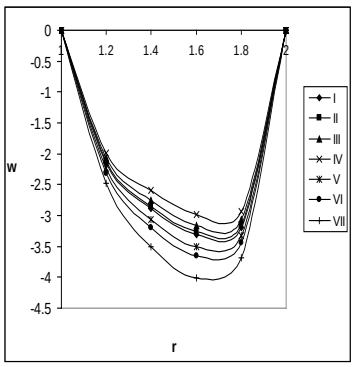

Fig. 4 : Variation of w withSc, γ

	I	II	III	IV	V	VI	VII	VIII
Sc	0.6	1.3	2.01	1.3	1.3	1.3	1.3	1.3
γ	0.5	0.5	0.5	1	2	-0.5	-1	-2

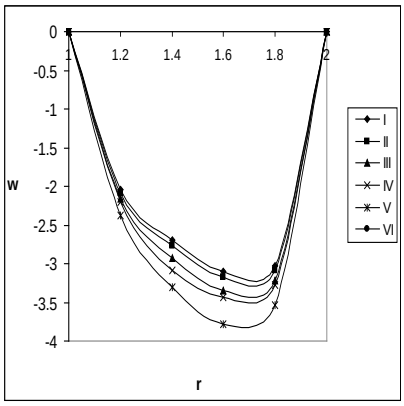

Fig.5:Variation of w with

	I	II	III	IV	V	VI
Q_1	0	0.5	1.5	2	4	6

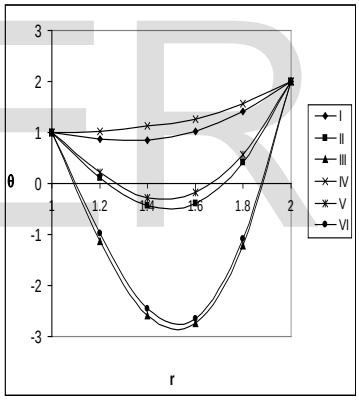

Q_1

Fig. 6 : Variation of θ with G

	I	II	III	IV	V	VI
G	10^2	$2x10^2$	$3x10^2$	-10^2	$-2x10^2$	$-3x10^2$

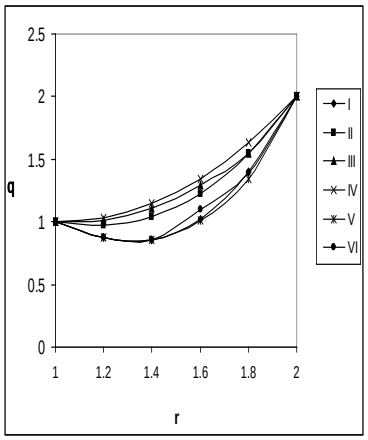

Fig. 7: Variation of θ with D^{-1}, M

	I	II	III	IV	V	VI
D^{-1}	10^2	$2x10^2$	$3x10^2$	$5x10^2$	10^2	10^2
M	2	2	2	2	4	6

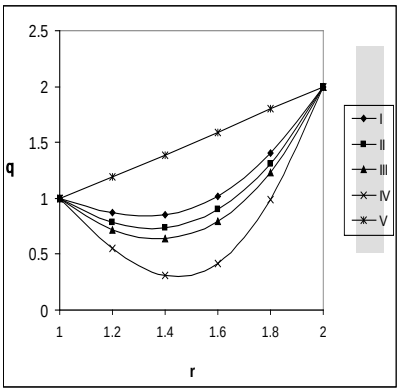

Fig. 8 : Variation of θ with α, N

	I	II	III	IV	V
α	2	4	6	2	2
N	1	1	1	2	-0.5

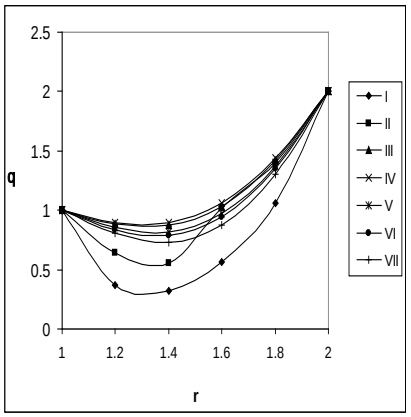

Fig. 9 : Variation of θ with Sc, γ

	I	II	III	IV	V	VI	VII	VIII
Sc	0.6	1.3	2.01	1.3	1.3	1.3	1.3	1.3
γ	0.5	0.5	0.5	1	2	-0.5	-1	-2

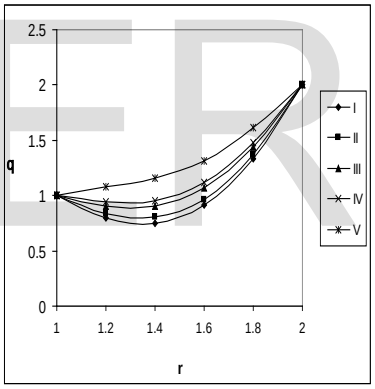

Fig. 10 : Variation of θ with Q_1

	I	II	III	IV	V
Q_1	0	0.5	1.5	2	4

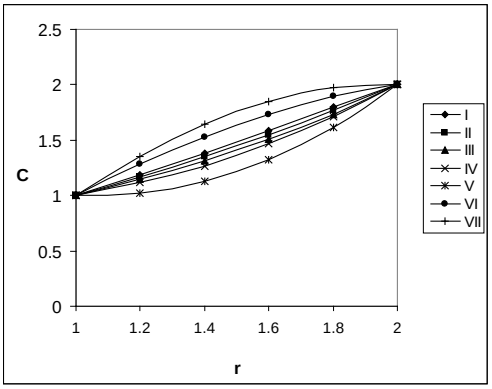

Fig.11: Variation of C with Sc, γ

	I	II	III	IV	V	VI	VII	VIII
Sc	0.6	1.3	2.01	1.3	1.3	1.3	1.3	1.3
γ	0.5	0.5	0.5	1	2	-0.5	-1	-2

Table – 1 Shear Stress (τ) at r = 1

G	I	II	III	IV
10^2	-6.0918	-4.60078	-3.321090	-4.34937
$3x10^2$	-18.38389	-14.15038	-10.19514	-13.27044
-10^2	6.00918	4.60078	3.32190	4.34937
$-3x10^2$	18.38389	14.15038	10.19514	13.27044
M	2	4	6	2
D^{-1}	10^2	10^2	10^2	$2x10^2$
Sc	1.3	1.3	1.3	1.3

V	VI	VII	VIII
-3.47856	-3.03905	-3.02403	-2.96897
-10.57694	-6.09571	-6.06550	-5.95584
3.47856	3.03905	3.02403	-2.6754
10.57694	6.09571	6.0550	5.95584
2	2	2	2
$3x10^2$	10^2	10^2	10^2
1.3	0.24	0.6	2.01

Table – 2 Shear Stress (τ) at r = 2

G	I	II	III	IV
10^2	8.17166	7.18271	6.12502	6.30307
$3x10^2$	25.06599	22.18817	18.93278	19.28109
-10^2	-8.17166	-7.18271	-6.12502	-6.30307
$-3x10^2$	-25.06594	-22.18817	-18.93278	-19.28109
M	2	4	6	2
D^{-1}	10^2	10^2	10^2	$2x10^2$
Sc	1.3	1.3	1.3	1.3

V	VI	VII	VIII
5.25561	4.14145	4.11884	4.03220
16.02143	8.30424	8.25877	8.08524
-5.25561	-4.14145	-4.11884	-3.99877
-16.02143	-8.30424	-8.25877	-8.08524
2	2	2	2
$3x10^2$	10^2	10^2	10^2
1.3	0.24	06	2.01

Table – 3 Shear Stress (τ) at r = 1

G	I	II	III
10^2	-6.00918	-5.67188	-5.42206
$3x10^2$	-18.38389	-17.27394	-16.46429
-10^2	6.00918	5.67188	5.42206
$-3x10^2$	18.38389	17.27394	16.46429
α	2	4	6

N	1	1	1

I	II	III
-4.51565	-0.71735	-0.26185
-9.06293	-1.44271	-0.53126
4.51565	0.71735	0.26185
9.06293	1.44271	0.53126
2	2	2
2	-0.5	-0.8

Table – 4 Shear Stress (τ) at r = 2

G	I	II	III
10^2	8.17166	7.70519	7.35129
$3x10^2$	25.06599	23.52506	22.37444
-10^2	-8.17166	-7.70519	-7.35129
$-3x10^2$	-25.06599	-23.52506	-22.37444
α	2	4	6
N	1	1	1

IV	V	VI
6.13833	0.98344	0.36540
12.31941	1.97210	0.73525
-6.13833	-0.98344	-0.36540
-12.31940	-1.97210	-0.73525
2	2	2
2	-0.5	-0.8

Table – 5 Shear Stress (τ) at r = 1

G	I	II	III	IV
10^2	-3.02122	-2.97138	-2.90453	-2.80755
$3x10^2$	-6.05983	-5.96070	-5.82618	-5.63142
-10^2	3.02122	2.97138	2.90453	2.80755
$-3x10^2$	6.05983	5.96070	5.82618	5.63142
γ	0.3	0.5	1.5	2.5

V	VI	VII	VIII
-3.10278	-3.13229	-3.26506	-3.47125
-6.22396	-6.28336	-6.55023	-6.96535
3.10278	3.13229	3.26506	3.47125
6.22396	6.28336	6.55023	6.96535
-0.3	-0.5	-1.5	-2.5

Table – 6 Shear Stress (τ) at r = 2

G	I	II	III	IV
10^2	4.11005	4.04192	3.94918	3.81380
$3x10^2$	8.24115	8.10473	7.91817	7.64612
-10^2	-4.11005	-4.04192	-3.94918	-3.81380
$-3x10^2$	-8.24115	-8.10473	-7.91817	-7.64612
γ	0.3	0.5	1.5	2.5

V	VI	VII	VIII
4.22195	4.26227	4.44235	4.71955
8.46629	8.54744	8.90970	9.46787
-4.22195	-4.26227	-4.44235	-4.71955
-8.46629	-8.54744	-8.90970	-9.46787
-0.3	-0.5	-1.5	-2.5

Table –7 Shear Stress (τ) at r = 1

G	I	II	III	IV
10^2	-2.97096	-3.12030	-3.31887	-3.51754
$3x10^2$	-5.95985	-6.25922	-6.65891	-7.05853
-10^2	2.97096	3.12030	3.31887	3.51754
$-3x10^2$	5.95985	6.25922	6.65891	7.05853
Q_1	0.5	2	4	6

Table –8 Shear Stress (τ) at r = 2

G	I	II	III	IV
10^2	4.04201	4.24537	4.51622	4.78718
$3x10^2$	8.10491	8.51341	9.05860	9.60398
-10^2	-4.04201	-4.24537	-4.51622	-4.78718
$-3x110^2$	-8.10491	-8.51341	-9.05860	-9.60398
Q_1	0.5	2	4	6

Table –9 Nusselt number (Nu) at r = 1

G	I	II	III	IV
10^2	0.59175	0.56355	0.54592	0.57703
$3x10^2$	0.48243	0.27736	0.20037	0.39073
-10^2	0.59175	0.56355	0.54592	0.57703
$-3x10^2$	0.48243	0.27736	0.20037	0.39073
M	2	4	6	2
D^{-1}	10^2	10^2	10^2	$2x10^2$
Sc	1.3	1.3	1.3	1.3

V	VI	VII	VIII
0.57222	0.61838	0.61265	0.59175
0.38831	0.60770	0.60213	0.58179
0.57222	0.61838	0.61265	0.589765
0.38831	0.60770	0.60213	0.58179
2	2	2	2
$3x10^2$	10^2	10^2	10^2
1.3	0.24	0.6	2.01

Table – 10 Nusselt number (Nu) at r = 2

G	I	II	III	IV
10^2	0.97953	1.00740	1.02471	0.98918
$3x10^2$	1.21358	1.43730	1.54759	1.27769
-10^2	0.97953	1.00740	1.02471	0.98918
$-3x10^2$	1.21358	1.43730	1.54759	1.27769
M	2	4	6	2
D^{-1}	10^2	10^2	10^2	$2x10^2$
Sc	1.3	1.3	1.3	1.3

V	VI	VII	VIII
0.99015	0.93807	0.94479	0.97030
1.26354	0.96081	0.96725	0.99172
0.99015	0.93807	0.94479	96.0345
1.26354	0.96081	0.96725	0.99172
2	2	2	2
$3x10^2$	10^2	10^2	10^2
1.3	0.24	0.6	2.01

Table – 11 Nusselt number (Nu) at r = 1

G	I	II	III
10^2	0.59175	-0.37042	-1.10500

$3x10^2$	0.48243	-0.42164	-1.12281
-10^2	0.59179	-0.37042	-1.10500
$-3x10^2$	0.48243	-0.42164	-1.12281
α	2	4	6
N	1	1	1

IV	V	VI
0.59764	0.60520	0.60537
0.57434	0.60463	0.60530
0.59764	0.60520	0.60537
0.57434	0.60463	0.60530
2	2	2
2	-0.5	-0.8

Table – 12 Nusselt number (Nu) at r = 2

G	I	II	III
10^2	0.97953	2.11236	3.03342
$3x10^2$	1.21358	2.27379	3.15007
-10^2	0.97953	2.11236	3.03342
$-3x10^2$	1.21358	2.27379	.15007
α	2	4	6
N	1	1	1

IV	V	VI
0.96689	0.95073	0.95037
1.01671	0.95198	0.95053
0.96689	0.95073	0.95037
1.01671	0.95198	0.95053
2	2	2
2	-0.5	-0.8

Table – 13 Nusselt number (Nu) at r = 1

G	I	II	III	IV
10^2	0.61155	0.59277	0.56716	0.53015
$3x10^2$	0.60106	0.58276	0.55780	0.52169
-10^2	0.61155	0.59277	0.56716	0.53015
$-3x10^2$	0.60106	0.58276	0.55780	0.52169
γ	0.3	0.5	1.5	2.5

V	VI	VII	VIII
0.64276	0.65405	0.70504	0.78365
0.63145	0.64243	0.69199	0.76825
0.64276	0.654050	0.70504	0.78365
0.63145	0.64243	0.69199	0.76825
-0.3	-0.5	-1.5	-2.5

Table – 14 Nusselt number (Nu) at r = 2

G	I	II	III	IV
10^2	0.94709	0.96777	0.99608	1.03727
$3x10^2$	0.96947	0.98925	1.01636	1.05586
-10^2	0.94709	0.96777	0.99608	1.03727
$-3x10^2$	0.96947	0.98925	1.01636	1.05586
γ	0.3	0.5	1.5	2.5

V	VI	VII	VIII
0.91287	0.90054	0.84524	0.76034
0.93680	0.92504	0.87237	0.79183
0.91287	0.90054	0.84524	0.76034
0.93680	0.42504	0.87237	0.79183
-0.3	-0.5	-1.5	-2.5

Table – 15 Nusselt number (Nu) at r = 1

G	I	II	III	IV

10^2	0.3271	1.17948	2.31515	3.45098
$3x10^2$	0.31780	1.16800	2.30154	3.43509
-10^2	0.32781	1.17948	2.31515	3.45098
$-3x10^2$	0.31780	1.16800	2.30154	3.43509
Q_1	0.5	2	4	6

Table – 16 Nusselt number (Nu) at r = 1

G	I	II	III	IV
10^2	1.26891	0.30316	-0.98449	-2.27221
$3x10^2$	1.29039	0.32741	-0.95628	-2.23976
-10^2	1.26891	0.30316	-0.98449	-2.27221
$-3x10^2$	1.29039	0.32741	-0.95628	-2.23976
Q_1	0.5	2	4	6

Table – 17 Sherwood number (Sh) at r = 1

Sc	I	II	III	IV
0.24	1.04479	0.68910	0.34352	-0.16133
0.6	0.96103	0.58765	0.32786	-0.1436
1.3	0.84567	0.48796	0.30786	-0.1231
2.01	0.67923	0.37896	0.22456	-0.1032
γ	0.3	0.5	1.5	2.5

V	VI	VII	VIII
-3.10278	-3.13229	2.17551	3.20499
-6.22396	-6.28336	2.17551	3.20499
3.10278	3.13229	2.17551	3.20499
6.22396	6.28336	2.17551	3.20499
-0.3	-0.5	-1.5	-2.5

Table – 18 Sherwood number (Sh) at r = 2

Sc	I	II	III	IV
0.24	0.80255	1.09567	1.50414	2.11563
0.6	0.6255	1.02337	1.3480	2.0569
1.3	0.5255	0.89765	1.2518	2.0056
2.01	0.3899	0.78654	1.2112	1.89763
γ	0.3	0.5	1.5	2.5

V	VI	VII	VIII
0.32633	0.15689	-0.58570	-1.69652
0.306778	0.1387	-0.4570	-1.5958
0.287659	0.1183	-0.58570	-1.3959
0.223567	0.0981	-0.58570	-1.11233
-0.3	-0.5	-1.5	-2.5

6. REFERENCES

1. Al. Nimir, M.A.: Analytical solutions for transient laminar fully developed free convection in vertical annuli., Int. J. Heat and Mass Transfer, V. 36, pp. 2388-2395 (1993).
2. Antonio Barletle.: Combined forced and free convection with viscous dissipation in a vertical duct., Int. J. Heat and Mass Transfer, V. 42, pp. 2243-2253 (1999).
3. Caltagirone, J. P.: J. Fluid Mech, V. 76, pp. 337 (1976).
4. Chen, T. S and Yuh, C. F.: Combined heat and mass transfer in natural convection on inclined surface. , J. Heat Transfer, V. 2, pp. 233-250 (1979).
5. Faces, N and Faroup, B.: ASME, J. Heat Transfer, V. 105, pp. 680 (1983).
6. Havstad, M. A and Burns, P.J.: Int. J. Heat and Mass Transfer, V. 25, No.1, pp. 1755, (1982).
7. Mihirsen and Torrance. K. E.: Int. J. Heat and Mass Transfer, V. 30, No. 4, pp. 729 (1987).
8. Nanda, R. S and Purushotham, R.: Int. Dedication seminar on recent advances on maths and applications, Varanasi (1976).
9. Neeraja, G.: Ph. D thesis, S.P. Mahila University, Tirupathi, India (1993).
10. Nguyen, T.H, Saish, M.G, Robillard and Vasseur, P.: ASME, The American Society of Mechanical Engineers, Paper No. 85-WA/HT-8, New York (1985).
11. Osterle, J. F and Young, F. J.: J. Fluid Mech. , V. 11, pp. 512 (1961).
12. Padmavathi, A.: "Finite element analysis of non – darcian convective heat transfer through a porous medium in

cylindrical& rectangular ducts with heat generating sources and radiation" Ph.D thesis, S. K. University, Anantapur, India (2009).
13. Philip, J. R.: Axisymmetric free convection at small Rayleigh numbers in porous cavities. Int. J. Heat and Mass Transfer, V. 25, pp. 1689-1699 (1982).
14. Poots, G.: Int. J. Heat and Mass Transfer, V. 3, pp.1 (1961).
15. Prasad, V.: Natural convection in porous media , Ph.D thesis , S. K.University, Anantapur, India (1983).
16. Prasad, V and Kulacki, F. A.: Int. J. Heat and Mass Transfer, V. 27,pp.207, (1984).
17. Prasad , V, Kulacki. F. A and Keyhari. M.: J. Fluid Mech., V.150, pp. 89 (1985).
18. Ravi, A.: Unsteady convection heat and mass transfer flow through aporous medium in wavy channels, Ph.D thesis, S.K.University, Anantapur, India (2003).
19. Robillard, L Ngugen, T, H, Sathish, M. G and Vasseur, P.: Heat transferinporous media and particulate flows, HTD-V. 46, pp. 41. ASM , (1985).
20. Sastri, V. U. K and Bhadram, C. V. V.: App, Sci. Res, V.34, 2/3. pp. 117 (1978).
21. Shaarawi, El. M. A. I and Al-Nimir, M. A.: Fully developed laminar natural convection in open ended vertical concentric annuli., Int. J. Heat and Mass Transfer , pp. 1873-1884 (1999).
22. Singh, K. R and Cowling, T. J.: Quart. J. Maths. Appl. Maths, V. 16, pp.1 (1963).
23. Sivanjaneya Prasad, P.: Effects of convection heat and mass transfer in unsteady hydromagnetic channels flow, Ph.D thesis, S.K. University, Anantapur, India (2001).
24. Sreenivas Reddy, B.: Thermo-diffusion effect on convection heat and mass transfer through a porous medium, Ph. D thesis, S. K. University, Anantapur, India (2006).
25. Sreevani, M.: Mixed convection heat and mass transfer through a porous medium in channels with dissipative effects, Ph.D. thesis, S, K. University, Anantpur, India (2003).
25a. Sudha Mathew.: Hydro magnetic mixed convective heat and mass transfer through a porous medium in a vertical channel with thermo-diffusion effect. Ph.D thesis, S,K. University, Anantapur, India (2009).
26. Sudheer Kumar, Dr.M.P.Singh, Dr.Rajendra Kumar.: Radiation effect on natural convection over a vertical cylinder in porous media., Acta Ciencia Indica, V.XXXII M, No.2 (2006).
27. Vassuer. P. Nguyen, T. H , Robillard and Thi, V. K. T.: Int. Heat and mass transfer , V. 27, pp. 337 (1984).
28. Whitehead, J. A.: Observations of rapid means flow produced mercury by a moving heater, Geophys Fluid dynamics, V. 3, pp. 161-180 (1972).
29. Yu, C. P.: Appl. Sci. Res, V. 22, pp. 127 (1970).
30. Yu, C. P and Yong, H.: Appl. Sci. Res, V. 20, pp. 16 (1969).
31. Sudha Mathew.: Hydro magnetic mixed convective heat and mass transfer through a porous medium in a vertical channel with thermo-diffusion effect. Ph.D thesis, S,K. University, Anantapur, India (2009).